

On an innovative deployment concept for large space structures

V. S. Zolesi¹ and P. L. Ganga²
Kayser Italia srl, Livorno, 57128, Italy

L. Scolamiero³
European Space Agency, ESA ESTEC, Noordwijk, 2200 AG, The Netherlands

A. Micheletti⁴ and P. Podio-Guidugli⁵
University of Rome TorVergata, Rome, 00133, Italy

G. Tibert⁶
KTH, Stockholm, SE-100 44, Sweden

A. Donati⁷ and M. Ghiozzi⁸
Kayser Italia srl, Livorno, 57128, Italy

Large deployable space structures are mission-critical technologies for which deployment failure cannot be an option. The difficulty to fully reproduce and test on ground the deployment of large systems dictates the need for extremely reliable architectural concepts. In 2010, ESA promoted a study focused at the pre-development of breakthrough architectural concepts offering superior reliability. The study, which was performed as an initiative of ESA Small Medium Enterprises Office (<http://www.esa.int/SME/>), by Kayser Italia at its premises in Livorno (Italy), with Universita' di Roma TorVergata (Rome, Italy) as sub-contractor and consultancy from KTH (Stockholm, Sweden), led to the identification of an innovative large deployable structure of "tensegrity" type, which achieves the required reliability because it permits a drastic reduction in the number of articulated joints in comparison with non-tensegrity architectures. The identified target application was in the field of large antenna reflectors. The project focused on the overall architecture of a deployable system and the related design implications. With a view toward verifying experimentally the performance of the deployable structure, a reduced-scale breadboard model was designed and manufactured. A gravity off-loading system was designed and implemented, so as to check deployment functionality in a 1-g environment. Finally, a test campaign was conducted, to validate the main design assumptions as well as to ensure the concept's suitability for the selected target application. The test activities demonstrated satisfactory stiffness, deployment repeatability, and geometric precision in the fully deployed

¹ President, V. Di Popogna, 501, 57128, Livorno, Italy, AIAA Senior Member, International Member of the LS&STC.

² Structural Manager, V. Di Popogna, 501, 57128, Livorno, Italy.

³ Senior Mechanical Engineer, Mechanical Engineering Department, European Space Agency – ESA/ESTEC Postbus 299, 2200 AG, Noordwijk, The Netherlands.

⁴ Assistant Professor of Strength of Materials, Department of Civil Engineering, V. del Politecnico, 1, 00133, Rome, Italy.

⁵ Professor of Strength of Materials, Department of Civil Engineering, V. del Politecnico, 1, 00133, Rome, Italy.

⁶ Associate Professor of Structural Mechanics, Department of Mechanics, SE-100 44, Stockholm, Sweden, AIAA Senior Member.

⁷ Marketing Director, V. Di Popogna, 501, 57128, Livorno, Italy.

⁸ Mechanical Engineer, V. Di Popogna, 501, 57128, Livorno, Italy.

configuration. The test data were also used to validate a finite element model, which predicts a good static and dynamic behavior of the full-scale deployable structure.

Nomenclature

n	=	number of bars in the Tensegrity Prism (TP)
a	=	lower TP “radius”
b	=	upper TP “radius”
h	=	TP height
φ	=	TP twist angle (for short, the twist)
h^*	=	“overlap” between two successive stages of a symmetric Snelson tower / Snelson Ring
γ	=	a/b ratio between the TP radii
δ	=	h*/h ratio between TP height and Snelson tower / Snelson Ring overlap
H_s	=	stowed height of the deployable tensegrity ring

I. Introduction

Large space antenna reflectors, with diameters between 4 and 25 meters, are required in several mission types, particularly in the telecommunication domain, but also for Earth observation, deep-space missions and radio-astronomy⁸.

Reflectors with diameter in excess of 4-5 meters must have a foldable structure, to be deployed once in orbit, for compatibility with the launchers’ available envelope. Demanding mechanical, thermal and radio frequency requirements of the as-deployed reflector, associated with the need for extreme deployment reliability, result in very challenging, multidisciplinary design issues. As a consequence, very few companies specialize in the production of such large reflectors, most of them being based in the US (Northrop-Grumman, Harris Corporation).

Aiming at reducing potential dependence on non-EU suppliers, ESA is pursuing developments in this domain. In particular, within the frame of an initiative of the ESA Small Medium Enterprises Office (<http://www.esa.int/SME/>), the study of a potentially breakthrough technology has been undertaken, whose goal was to conceive a deployable large antenna reflector of intrinsically high reliability. A concept validation by testing a reduced-scale breadboard model has been performed.

This paper reports the outcome of the above mentioned activities, namely, the conception of an innovative large deployable structure based on “tensegrity” principles, currently being protected by an international patent filing¹⁵.

II. Large Space Deployable Reflectors

The need for large antenna reflectors of 4-25 meters in diameter is well established⁸; in fact, the market goes beyond pure telecommunication missions (still the major users of such technology), and spans from Earth observation, navigation, and deep-space missions, to radio-astronomy.

Operative radio frequency bands go from the lowest P-band frequencies up to the L-S, Ku and higher, and finish with the Ka band, this last band being reserved to small-diameter reflectors.

Several 12-meter reflectors have already successfully flown, and recent missions have embarked and successfully deployed reflectors up to 18 and 22 meters in diameter.

To comply with the demanding radio frequency needs, as-deployed shape accuracy and high stability in operational conditions (for the entire operational life) are required. To limit the overall reflector mass, high-stability / low-density materials and technologies are utilized, with large use of Carbon Fiber Reinforced Plastics (CFRP) for rigid structural members. Subtler radio frequency phenomena (known as Inter Modulation Products) pose even more challenging requirements and restrictions, both on candidate materials, and process selection and on thermo-mechanical design solutions.

But what makes antenna reflectors unique in terms of design challenges is the need for extreme deployment reliability: a deployment failure would most of the times result in the loss of mission, an unacceptable option.

Several concepts have been studied worldwide to combine the reflector-specific set of multidisciplinary requirements and the fundamental need of an absolutely reliable deployment. However, the very specialized competency required, and the amount of investment necessary to develop/qualify reliable products, have resulted in very few companies offering commercially qualified units, the most prominent being Harris Corporation¹² and Northrop-Grumman¹³.

The experience gained by the major large reflector suppliers notwithstanding, the deployment of such items is always a critical step in a mission scenario. Indeed, the typical structure to be deployed consists of a large number of interconnected rigid elements. As a consequence, a large number of mechanical joints (either simply revolute or telescopic, or motorized, joints) are necessary to fold the structure when in launch configuration and to deploy it in orbit.

Mechanical joints / hinges, and “mechanisms” in general, are typically sources of reliability concern, in that they may induce localized failures. The starting point of the development presented in this paper is that a “joint-free” system, or at least one with a minimal number of joints, would offer superior reliability performance, being “intrinsically” free of single-point failure sources.

The possibility of using a structural architecture of “tensegrity” type, where mechanical joints are in principle totally absent from the design, was then considered. The idea of using “tensegrity”-type structures for large antenna applications is not new, and in fact it has been the subject of a related patent¹⁶. However, it is our opinion that the new ideas we conceived in the course of our study, and the new design features we introduced, make the final design original and unique, so much so as to deserve an international patent filing¹⁵.

In the following sections, we shall describe the technical features of the structural architecture we propose, as well as its validation by means of the realization of a scaled model breadboard and a test campaign.

III. Tensegrity Structure Description

A. Definition

Tensegrity Structures (TS) were invented in 1948 by the artist Kenneth Snelson¹. In the 1960’s, Snelson began to build a number of outdoor sculptures, which made tensegrities worldwide popular among architects and engineers because of their innovative structural concept. Indeed, when an architect or a structural engineer looks at a realization of Snelson’s, he observes that:

- TS’s are prestressed spatial *frameworks whose elements are bars and cables*;
- the cable collection is a connected set (*tensile-integrity*);
- bar ends never touch (floating compression).

In addition, TS’s possess the important *form-finding property*, to be described in Section III C.

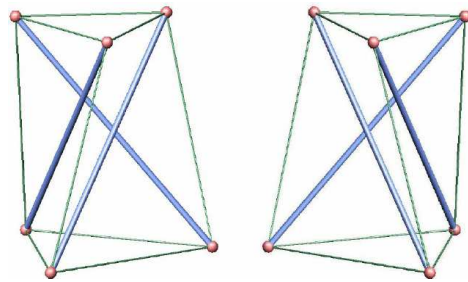


Figure 1. The simplest three-dimensional TS. Tensegrity prisms with opposite orientations.

B. The Tensegrity Prism

A regular n -bar Tensegrity Prism (TP) is a cyclic-symmetric structure with an n -fold axis of cyclic-symmetry, which one always assumes to be vertical.

As shown in Fig. 1, a TP can have two different orientations.

The geometry of a TP can be identified by means of five parameters (Fig. 2):

- the number of bars n ,
- the lower “radius” a ,
- the upper “radius” b ,
- the height h , and
- the twist angle φ (for short, the twist φ).

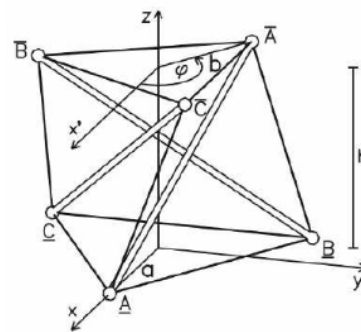


Figure 2. The TP parameters.

C. Form-finding property

As observed by Oppenheim and Williams⁵ (1997), form-finding (FF) is a property that becomes evident when we try to build a TS by hand. Let us suppose that we have what is necessary to assemble the system in Fig. 1, all the elements having a fixed length. Once all the connections between elements but the last one are realized, we notice that the partial assembly we obtained has no stiffness and that there are many possible configurations with slack

cables. The length of the last element is determined when we try to decrease (increase) the distance between the two nodes to be connected if the last element is a cable (a bar). That distance varies until it reaches a minimum (maximum) value, at which the system takes its shape. If we force the two nodes to get closer (farther), then the system acquires a self-stress state with the last element in tension (compression). Figure 3 illustrates the FF property in the simplest case. With this example in mind we can state the FF property as follows: “Given a N -elements tensegrity system, if the lengths of $(N - 1)$ elements are fixed, then a stable equilibrium configuration is obtained when the last cable (bar) has minimal (maximal) length.”

For a fixed topology, i.e., once a collection of nodes connected by bars and cables is chosen, it is possible to pass from one stable configuration to another simply by changing the lengths of two or more elements.

Due to the FF property, a tensegrity system is stable only for a restricted set of configurations. For example, in the system in Fig. 3, such restriction corresponds to requiring that the three nodes be collinear. The problem of finding the set of stable configurations for a given tensegrity system, referred to as “form-finding problem”, has been extensively studied in the literature^{3,4}.

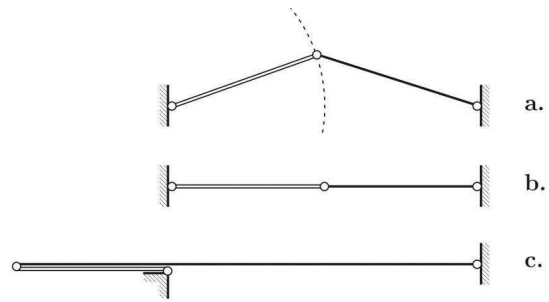


Figure 3. Form-finding property. The form finding property for a system composed of two elements. The double line element has fixed length; the single line element has variable length. The central node can only be on the dashed circumference shown in a. Let's suppose we progressively shorten the single line element, we will reach configuration b; if we try to shorten this element more, a self-stress state will be established with this element in tension. Analogously, the same element can be lengthened until we reach placement c; in the same way this element can be forced in compression

D. Tensegrity Deployable Structures

The FF property of tensegrity systems, together with their related ability to change shape, suggests using these systems when it is desirable to have deployable or variable-geometry structures, or smart structures, some elements of which serve as sensors and actuators. By actuating cables and/or bars, a TS can pass from one equilibrium configuration to another through a continuous path of equilibrium configurations (Fig. 4 shows a TS ring in different equilibrium configurations). Due to the absence of hinges between bars, the mechanical behavior of a floating-compression system can be predicted with better accuracy than for conventional hinged systems.

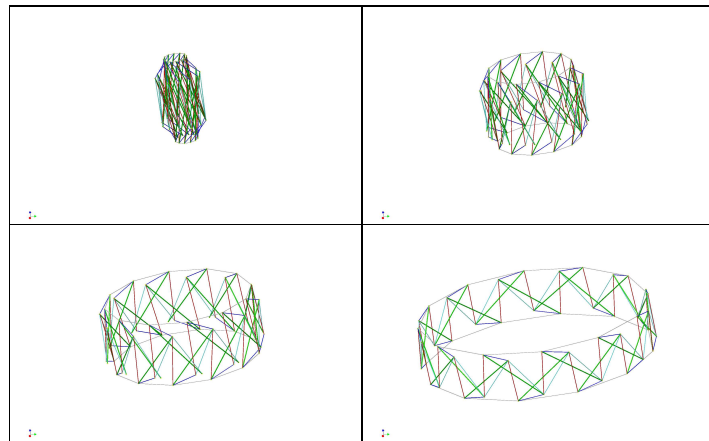


Figure 4. TS ring in different equilibrium configurations.

E. Tensegrity Rings for Space Structures

The first studies of ring-shaped TS's appear to be performed by Burkhart¹¹ in 2003; a tensegrity torus is analyzed in Peng⁶ et al. (2006) and Yuan² et al. (2008).

The Tensegrity Ring (TR) concept is suitable for disc- or ring-shaped Space Structures. Since bars are not connected to each other, none of the usual hinge mechanisms are present in TS's: freedom in spatial orientation and relative motion of bars during deployment is granted, due to the flexibility of the interconnecting cables. The absence of mechanical joints drastically reduces the possible failure modes of the deployable system, thus increasing its overall reliability, a fundamental requirement for this type of space technology; in addition, this feature permits

an especially tight and compact stowage of the structure. Moreover, as for conventional pin-jointed trusses, none of the individual members is bent, sheared or twisted.

We named the tensegrity ring we developed for the present application “Snelson Ring” (SR). SR is a TR with the same graph as a two-level Snelson tower. To obtain a Snelson tower, we “superimpose” a number of Tensegrity Prisms (TP) (as shown in Fig. 1) by repeating the following sequence of steps:

- 1) We take two prisms with opposite orientations
- 2) We remove the lower cables of the upper prism
- 3) We connect the lower nodes of the upper prism with the middle points of the upper base cables of the lower prism
- 4) We add $2n$ additional cables (in green in Fig. 5)

In a SR, we distinguish four groups of cables according to position, in such a way that symmetrically placed cables belong to the same group. The cables in these groups are named as follows:

- “verticals”, connecting bars of the same TP;
- “diagonals”, connecting bars of different TP’s;
- “saddles”, belonging to both TP’s;
- “polygonals”, forming base polygons.

Verticals, diagonals and saddles are depicted in Fig. 5 respectively in blue, green and red.

The geometry of symmetric Snelson towers can be identified by six parameters, namely, the above-defined five parameters (n, a, b, h, φ) of a typical TP plus a new parameter:

h^* = the “overlap” between stages (see Fig. 5).

Note h^* is null when saddles lay on the same horizontal plane. Three additional geometric properties are used to characterize a deployable SR:

- δ = the overlap ratio (h^*/h) between the Snelson tower / Snelson Ring overlap and the TP height;
- γ = ratio (a/b) between the two radii of the typical TP;
- H_s = stowed height of the deployable tensegrity ring

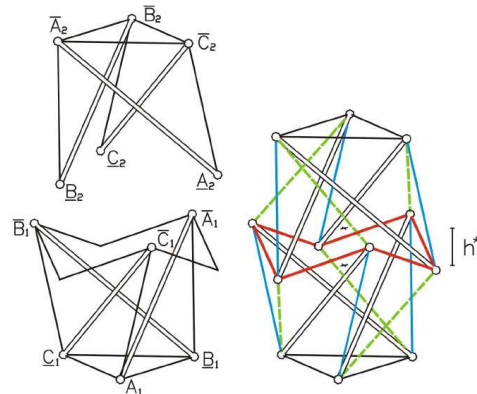


Figure 5. Superposition of two Tensegrity Prisms (TPs) to obtain a two-level Snelson Tower.

F. Deployment strategy

A TR can be deployed by changing the length of some of its elements so as to obtain the desired change in shape from stowed to deployed configurations. For the SR considered for the present application, it was chosen to change the length of a subset of cables, while keeping constant the lengths of the remaining ones and that of all the bars. In order to have a slow, smooth and controllable deployment process, all the cables in the TR have to be kept in tension. The adopted deployment strategy consists of two phases:

- the change in configuration, from folded to deployed (Deployment Phase 1);
- the final pre-stressing, to reach a prescribed stress level in the system (Deployment Phase 2).

1. Deployment Phase 1

During Phase 1 of deployment, the change of configuration is obtained by changing only the lengths of two group of cables: the polygonal cables lengthen, the vertical cables shorten. Figure 6 shows the stowed and the deployed configuration of a hexagonal TR, one obtained from the other in this way.

2. Deployment Phase 2

Due to the FF property, the pre-stress can be induced in the structure by acting on few cables only. These cables can be conveniently chosen among those not involved in Phase 1, since the corresponding actuators will apply a large force to obtain a small change in length.

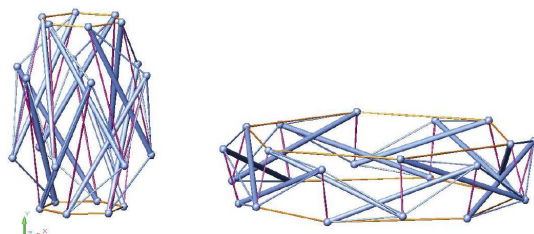


Figure 6. Hexagonal TR folded and deployed. Red cables are shortened during deployment. Yellow cables are lengthened during deployment.

IV. Tensegrity Space Structure Design

A deployable tensegrity ring of Snelson type (SR) was identified as the main structure in a Tensegrity Space Structure (TSS) to be designed consistent with the following specifications, among others:

- Function: Deployable Antenna Reflector
- Operating frequency: from 6 to 14 GHz
- Reflective Mesh tension: 5 N/m
- Reflector diameter: 12 m
- Stowed height: about 4.4 m
- Stowed diameter: about 1.2 m (excluding the reflector to boom interface)
- Mass budget: 57 kg or less (excluding the spacecraft boom)
- Eigenfrequency (deployed, not including boom): 1.2 Hz (min), 1.5 Hz (target)

The considered specifications take into account the typical launcher mechanical interface (i.e. stowed dimensions) and the typical ratio between deployed diameter and folded diameter.

A. Tensegrity Ring Analysis

A parametric analysis of the SR⁹ was performed in the absence of the inner tension truss (also called web in the present document).

An FF analysis showed that suitable configurations have a small twist φ and a large overlap ratio δ . Note that it is not possible to have $\delta \geq 1$, since this would require that some cables take a compressive stress; moreover, having $\gamma > 1$ causes problems with regard to the clearance between bars. Given these constraints, we focused on those configurations having γ close to, but not greater than 1. To pick a convenient set of geometric parameters, we looked at deployability, in particular, we computed an approximate value of the

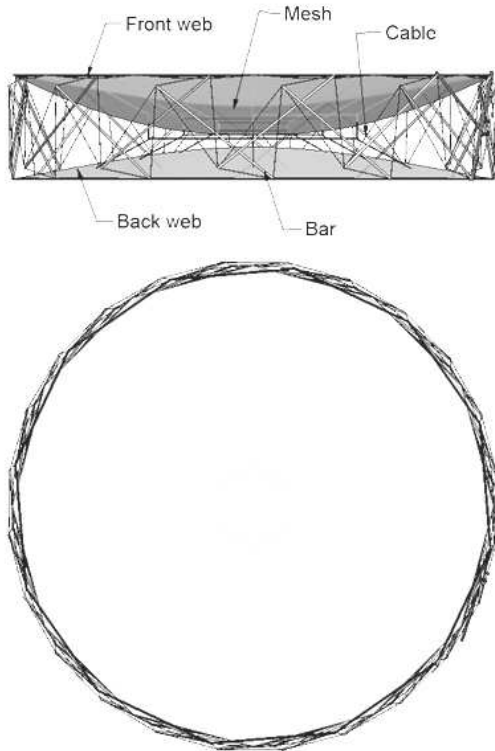


Figure 8. TSS Flight Model Deployed. TSS to Boom I/F not shown in the picture.

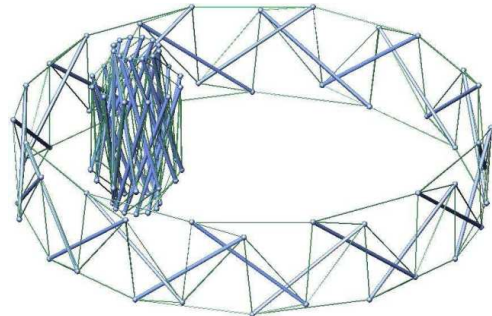


Figure 7. TSS Deployable Tensegrity Ring model.

Folded and deployed configurations.

Parameters: $n = 12$, deployed diameter = 12 m, deployed height = 2.6 m, $\varphi = 28^\circ$, $\gamma = 0.98$.

Resulting $H_s = 4.53$ m

stowed height H_s , as the sum of the lengths of one bar and one diagonal cable. We did this because in the stowed configuration these elements, which are kept almost parallel to the vertical axis, span the height of the SR. The computed values showed that the stowed height requirement can be fulfilled. However, a precise computation using a finite element model gives smaller values of H_s only for $\gamma = 1$; by taking $\gamma = 0.98$, it is possible to obtain a H_s value around 4.5 m. The following parameters were chosen in order to provide a compact stowage of the ring: $n = 12$, a deployed diameter of 12 m, a deployed height of 2.6 m, $\varphi = 28^\circ$, $\gamma = 0.98$; the resulting stowed height is $H_s = 4.53$ m. Figure 7 shows such an SR both folded and deployed.

B. Flight Model design

A preliminary design of the Flight Model of the TSS was performed, with the aim of investigating the expected physical and structural properties of the TSS when materials easily available on the market are used.

The Flight Model is composed of the following elements: cables, bars, front and back web (in light gray in Fig. 8), reflective mesh (in heavy gray), deployment actuation system, tensioning actuation system, and TSS-to-boom (spacecraft) apparatus I/F.

Figure 8 shows some of the above mentioned elements. The Flight Model is 12 m in diameter and 2.6 m in height in its deployed configuration, 2.33 m in diameter and 4.53 m in height when folded.

All the 24 TSS TR bars are of the same fixed length. The overall calculated mass is 58 kg, including all the above mentioned elements and an additional 10% margin to take into account unavoidable uncertainties at this stage of design.

The front and back webs are fastened to the top and bottom polygons of the TR; moreover, they are linked to each other by means of tension elements, called tension ties. The reflecting mesh is fastened to the top web by means of tension elements distributed all over its surface, so as to give it the required working shape.

The TR is composed of groups of cables identified as specified in Section III E and shown in Fig. 9. Notice the additional group consisting of two continuous cables, henceforth referred to as the hoop cables, running in parallel to the top and bottom polygons, whose service function is explained below.

Recall that some of the cables maintain a fixed length both in stowed and in deployed configuration (except of course for the modest lengthening due to tension), while other cables change their length during deployment: some become longer, others shorter: precisely, vertical cables shorten during structure deployment, and hoop cables lengthen. The “shortening” of a vertical cable is obtained by pulling it inside a bar tube, by means of the deployment passive actuator described below; the cable portion remaining outside the bar after shortening is visible in Fig. 9.

The two hoop cables, the one running through the top-polygon nodes and the other running through the bottom-polygon nodes, are lengthened by unwinding them from pulleys driven by electrical motors (the deployment active actuators) with controlled speed. Their function is to regulate the deployment speed during Phase 1 of deployment: at the end of Phase 1 of deployment, they become slack and have no structural role in the fully deployed configuration. On the contrary, polygonal cables are slack during the Phase 1 of deployment and become in tension at the end of Phase 1 of deployment. They inherit the structural role of the hoop cables, starting from Phase 2 of deployment and, later, in the fully deployed configuration. Note that polygonal and hoop cables appear overlapped in Fig. 9.

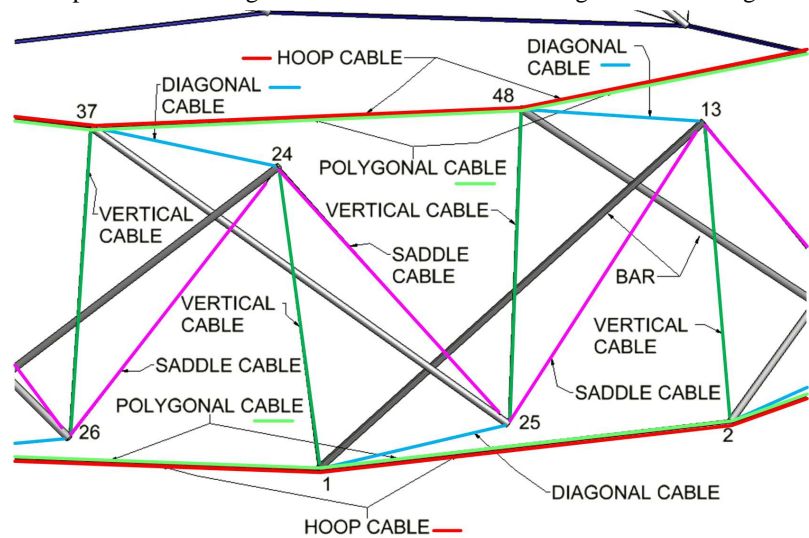


Figure 9. TSS cables nomenclature. Close-up view of a portion of the TSS.

Finally, diagonal and saddle cables are always (that is, in the folded and deployed configurations, and during deployment) in tension.

The two deployment phases are implemented by means of the actuation systems mentioned above. Deployment Phase 1 is implemented by means of both the passive and the active actuators. There are 24 passive deployment actuators (one inside each bar), which pull vertical Cables inside bar tubes; by means of pre-loaded springs, they provide the force needed during Phase 1. Each of the two active deployment actuators consists a rotating electrical motor and a pulley, where a hoop cable is coiled in the folded configuration. These actuators unwind the hoop cables during Phase 1; they make sure that deployment proceeds in a smooth way, and reduce the deployment speed. In fact, in the absence of the active actuators, Phase 1 would last

Finally, diagonal and saddle cables are always (that is, in the folded and deployed configurations, and during deployment) in tension.

The two deployment phases are implemented by means of the actuation systems mentioned above. Deployment Phase 1 is implemented by means of both the passive and the active actuators. There are 24 passive deployment actuators (one inside each bar), which pull vertical Cables inside bar tubes; by means of pre-loaded springs, they provide the force needed during Phase 1. Each of the two active deployment actuators consists a rotating electrical motor and a pulley, where a hoop cable is coiled in the folded configuration. These actuators unwind the hoop cables during Phase 1; they make sure that deployment proceeds in a smooth way, and reduce the deployment speed. In fact, in the absence of the active actuators, Phase 1 would last

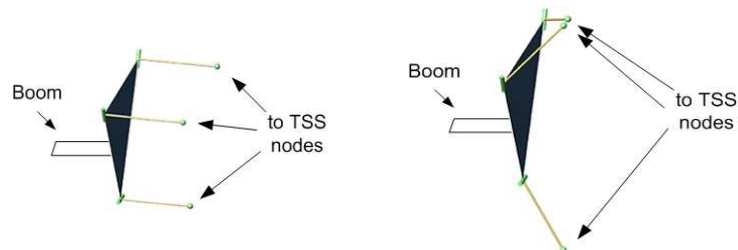


Figure 10. TSS to Boom I/F. Left: deployed configuration; right folded configuration

only a few seconds, due to the action of the pre-loaded springs, and could cause uncontrolled perturbations not only of the TSS but also of the spacecraft. Phase 1 ends when passive actuators have come to the end of their strokes, locking devices have reached the locked position, and hoop cables are completely unwound (at the end of Phase 1, the locking devices fix the position inside the bars of the endpoints of vertical cables, henceforth keeping their length fixed).

At the end of Phase 1, the TSS has shape and dimensions close to the final ones; however, its stiffness is still low, because the cables do not have the design tension yet, placed during Phase 2, by means of specific actuators. Three tensioning actuators are mounted 120° apart in the top polygon, so as to apply the required tension to three of the diagonal cables, and hence to all the dependent cables. Tensioning actuators apply tension by reducing the distance between the points to which the diagonal cables are fastened. As a consequence, during Phase 2 of deployment the TSS geometry is slightly modified.

The TSS Flight Model is attached to the spacecraft boom by means of an interface structure denoted by I/F, consisting of a plate (where the boom is attached) and three arms connected to three nodes of the TSS. Three cylindrical hinges and three spherical hinges are used to connect the arms to the plate and to the TSS (see sketch in Fig. 10).

The two active deployment actuators that unwind the hoop cables during Phase 1 are also mounted on the I/F.

An important role in the TSS functions is assigned to the reflective mesh and to the web. The material of choice for the radio frequency (RF) reflective surface must have low density and be easily foldable into a compact shape. The most common surface material for space reflectors of moderate precision is a mesh knitted from metallic or synthetic fibers plated with RF reflective material. The mesh must be sufficiently compliant to match without wrinkling the web's doubly curved surface. As the most recent studies suggest⁷, 5 N/m is a mesh-tension value sufficient for operating frequencies up to 14 GHz. Since earlier studies also find this value suitable, we selected it as the nominal tension in the reflective mesh of our antenna. The relevant web configuration was analyzed (dimension of triangle sides and web tension, see Fig. 11). The tension-truss concept requires that the triangulated web is put under tension by loads approximately perpendicular to the surface of the antenna. The tension-truss concept is used in several antennas, currently

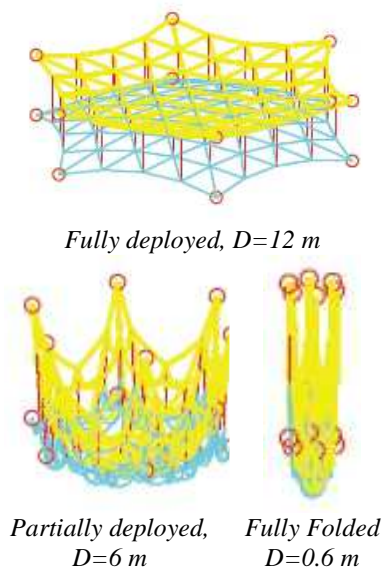


Figure 11. Simulation of the RF mesh supporting web configuration. Web in different deployment steps. Red lines represent the Tension-ties.

operating in orbit. Its main advantage is in the easy way the paraboloidal surface can be adjusted so as to increase its geometric accuracy without any need to change the configuration of the supporting ring structure. The configuration of tension ties for the TSS was analyzed (e.g., axial / non-axial tension ties), and deployment simulations were performed. The analyses suggested to avoid non-axial tension ties. To conform to the no-elongation and easy-tensioning requirements, a tension-tie configuration was identified and studied for a five-ring web assembly. This solution, which is in our opinion the simplest one, can be adopted also for a larger number of rings.

Mesh folding and stowage is critical and shall be studied in detail, as for state-of-the-art large reflectors. Mesh development activity foresees test to characterize mesh mechanical properties including tendency to self-adhesion. The absence of external mechanical joints is considered advantageous also in relation to reduced risk of mesh entanglement.

The launch regime will be addressed by designing suitable Hold-down and release system for the deployable boom plus reflector dish assembly. There will be primary hold-down mechanisms to hold-down the deployable boom to the spacecraft lateral panel, and secondary hold-down mechanisms to restrain the reflector dish in its folded state and release it when boom deployment has been completed.

In Europe ESA⁸ has already pre-qualified a deployable boom system with

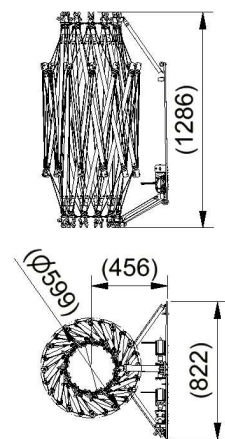


Figure 12. TSS BB Dimension (mm). The web is not shown in this picture.

associated motorized deployment mechanisms and hold-down release system for a large reflector antenna of 12 m aperture. The challenge of reflector dish to deployable boom mechanical connection has been addressed and included in the present development.

C. Breadboard design

We performed a detailed design of a breadboard (BB) having all of the main structural features of the Flight Model described above. The Breadboard was manufactured and tested as described below.

The TSS Breadboard is composed of the following main components: cables, bars, a simplified web consisting of radial cables, deployment actuation system, tensioning actuation system, TSS-to-Boom I/F. The BB is a scaled version of the TSS Flight Concept, designed according to the following rules:

- the polygon has the same number of sides (12) as the Flight Concept;
- the scaling ratio 1:4 applies to the overall deployed dimensions;
- the dimensions of the components (e.g., joints, cable and bar cross-sections) may not be equally scaled.

The rigid parts of the BB were made mainly of aluminum and stainless steel; for cables Vectran® was used; cables terminals were realized with the use of thimbles and ferrules.

Bars are composed of a tube and two joints, one for each bar end. The two joints of a bar are obtained by assembling machined parts, and include the interfaces between that bar and all the relative cables. Each bar includes, inside the tube, a passive deployment actuator, used to shorten a vertical cable. Such an actuator pulls inside the bar a portion of the cable, shortening the cable portion external to the bar. During deployment, the cable is retracted into the bar, so that the distance between the two bars connected by that cable is reduced (for these reason, such a cable is also referred to as a shortening cable). The 24 passive actuators inside the bars provide, by means of compression springs, the force needed to deploy the

structure in the course of the Phase 1. Each passive actuator includes a locking device, which is needed to lock the shortening cable (vertical cable), into position and to fix its length, when Phase 1 has been completed. The two joints located at a bar's ends are different, because the cables they join have different roles, and also because, there is a cable that enters the bar tube at only one of the bar's two ends. This cable is pulled by the passive actuator during deployment. The two joints are called joint A and joint B, with the cable being retracted into joint B.

The BB web consists of two sets of radial cables, joining the top-polygon vertices with the top-polygon center point and the bottom-polygon vertices with the bottom-polygon center point. Two discs collect, respectively, the top radial and the bottom radial cables; they are connected by an elastic member called a tension tie (see Fig. 15).

The BB was provided with a gravity compensation system (GCS), to reduce gravity effects as much as possible during deployment. The GCS is composed of an aluminum plate, called GCS plate, fixed to the ceiling of the laboratory, and of the cables by which the BB is attached to the GCS plate.

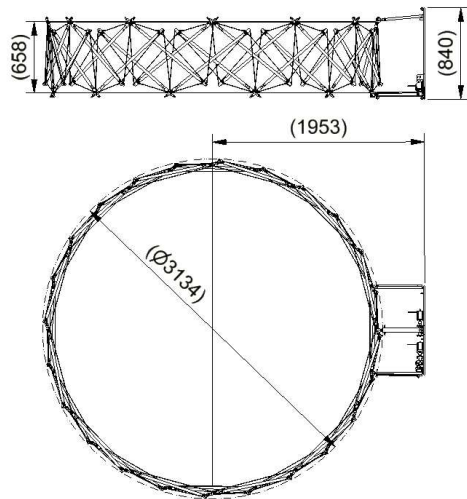


Figure 13. TSS BB Deployed Dimension (mm).

The web is not shown in this picture.

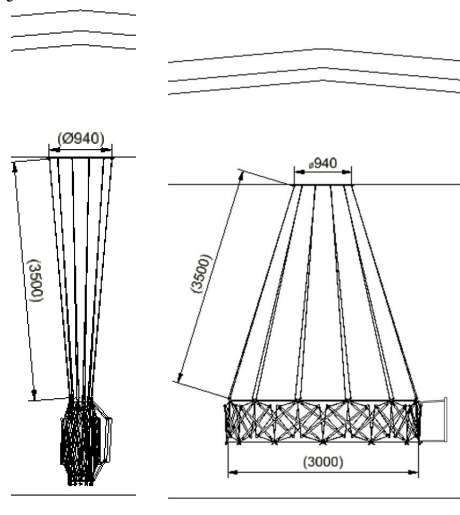


Figure 14. TSS BB attached to the GCS. Left: folded, right: deployed

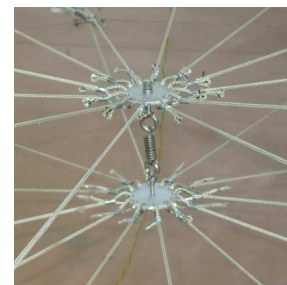


Figure 15. TSS BB Web. A single tension-tie is present including a spring (between the top and bottom centers)

12 out of 24 of the BB Bars are attached to the GCS plate. The three tensioning actuators and the TSS-to-Boom I/F are also attached to the GCS plate. The TSS-to-Boom I/F is attached to the GCS plate by means of three cables. GCS cables are composed of series of springs and a rope cable (of the same material used for the BB cables). The number and the elastic properties of the springs are selected so as to decouple the natural frequency due to GCS cables from the natural frequency of TSS ring (in particular, the springs that equip the suspension cables provide a natural frequency of about 0.5 Hz in the vertical direction). Figure 14 shows the BB attached to the GCS; the relevant reference dimensions are indicated; it is also shown how the TSS-to-Boom I/F modifies its shape on unfolding.

In the unfolded configuration, the horizontal component of the GCS constraining force applied to the BB ring is about 20% (peak value) of the vertical one. A moving mass is used to compensate the radial component of the TSS-to-Boom I/F weight force.

V. Breadboard Test Campaign

A test campaign was performed on the breadboard described above, including:

- 1) BB Geometry and Shape Test;
- 2) BB Performance Test (deployment and folding-up);
- 3) BB Structural Test (stiffness);
- 4) BB Stop-and-Go Test.

Figure 16 and Fig. 17 show the TSS BB attached to the GCS cables. On the left is visible the TSS-to-Boom I/F.

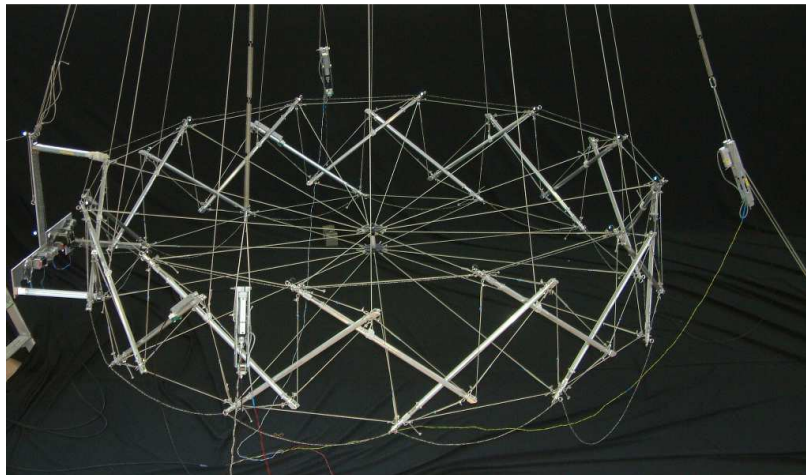


Figure 16. TSS BB attached to the GCS. *Deployed configuration – top-side view*

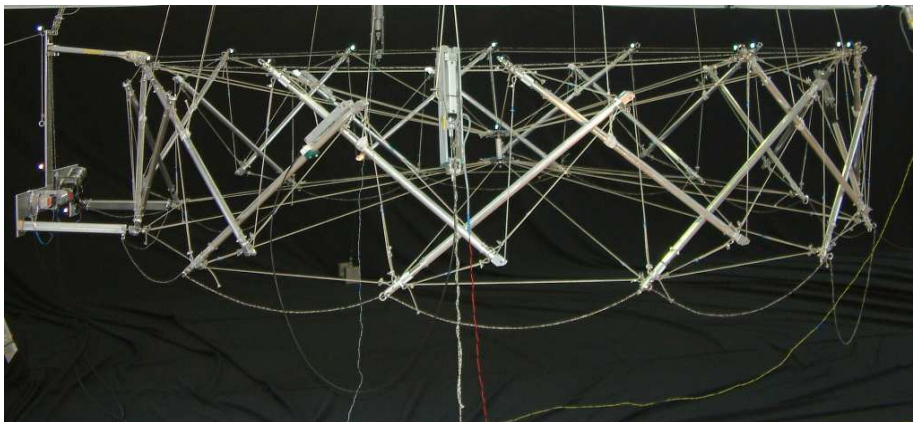


Figure 17. TSS BB attached to the GCS. *Deployed configuration – side view*

A. BB Geometry and Shape Test

This test was aimed at measuring the geometrical-shape repeatability of the structure in the deployed configuration. The position of some points of the deployed structure after different stowing/deployment sequences was measured and the relevant differences in position between one stowing/deployment sequence and the others were calculated (post-processing). Three folding / deployment sequences were performed and the geometry data acquired (3 repetitions).

A total station (laser measurement) was used to acquire the position of 15 markers placed on the BB.

The data were elaborated in two ways:

- 1) Calculating the distances of all the marker pairs and the relevant statistics (mean and standard deviation). The calculated mean of the standard deviation for markers located on the top polygon's sides was 0.34 mm.
- 2) Calculating by orthogonal regression the fitting planes for markers placed on the TR top polygon's nodes. For the point distances from the fitting plane calculated for the three acquisitions, this elaboration showed a variance between 0.03 and 0.36 mm² and a standard deviation between 0.16 and 0.6 mm.

All in all, the test showed a good repeatability of the folding/deployment process.

B. Breadboard Performance Test

The aim of this test was to verify that the deployment of the structure worked smoothly, with no bar and/or cable entanglements. Five folding/deployment complete sequences were performed. An entanglement occurred only during sequence no. 4, due to the wrong folding of one of the cables that prevented complete deployment.

C. Breadboard Structural Test and analysis

The aim of this test was to measure the natural frequencies of the BB.

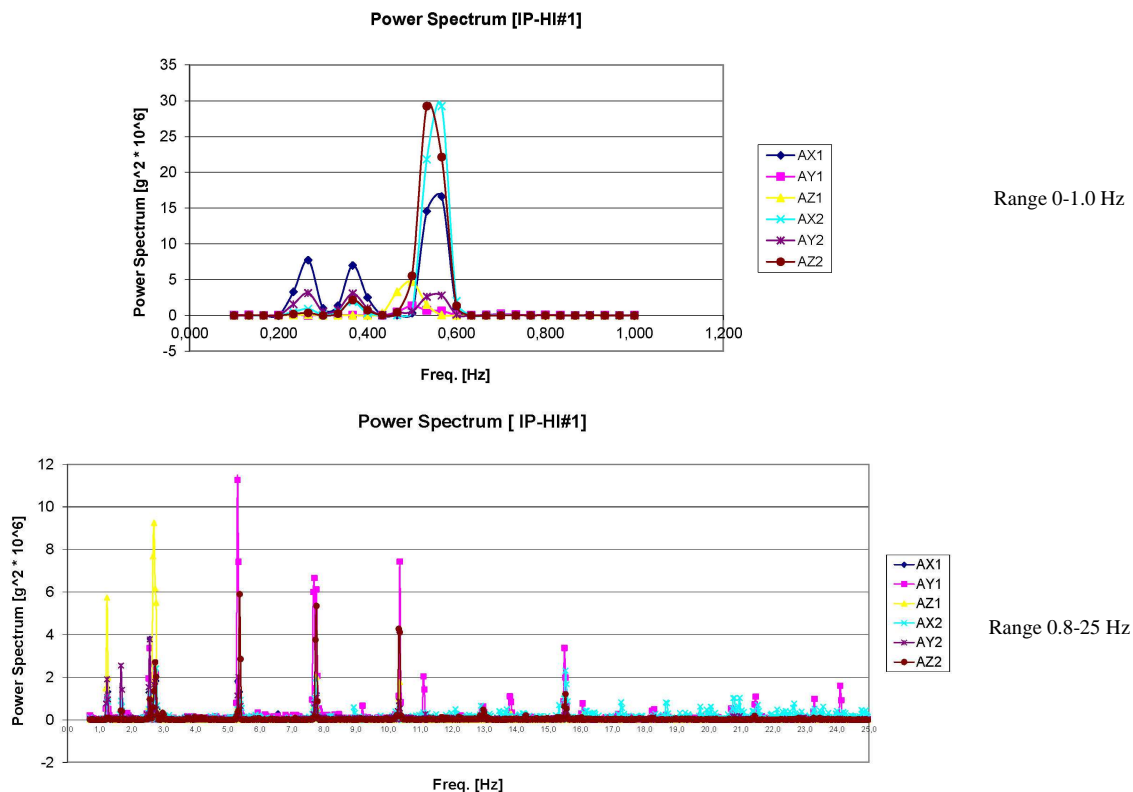


Figure 18. TSS BB - Recorded power spectrum vs. frequency. In-plane perturbation.

Two tri-axial accelerometers were placed on the structure and the response to in-plane and out-of-plane perturbations of the ring was recorded. The in plane perturbation was introduced by means of a rope passing through diametrically opposite bars ends of the top and bottom polygons. The rope length was such to reduce the diametrical distance of the connected bar ends (i.e. ring forced to an elliptical shape). The rope was then cut causing the

perturbation in the radial direction. The out-of-plane perturbation was introduced constraining to the ground a bar end of the ring structure, so to force the ring to a cantilever-like bent shape.

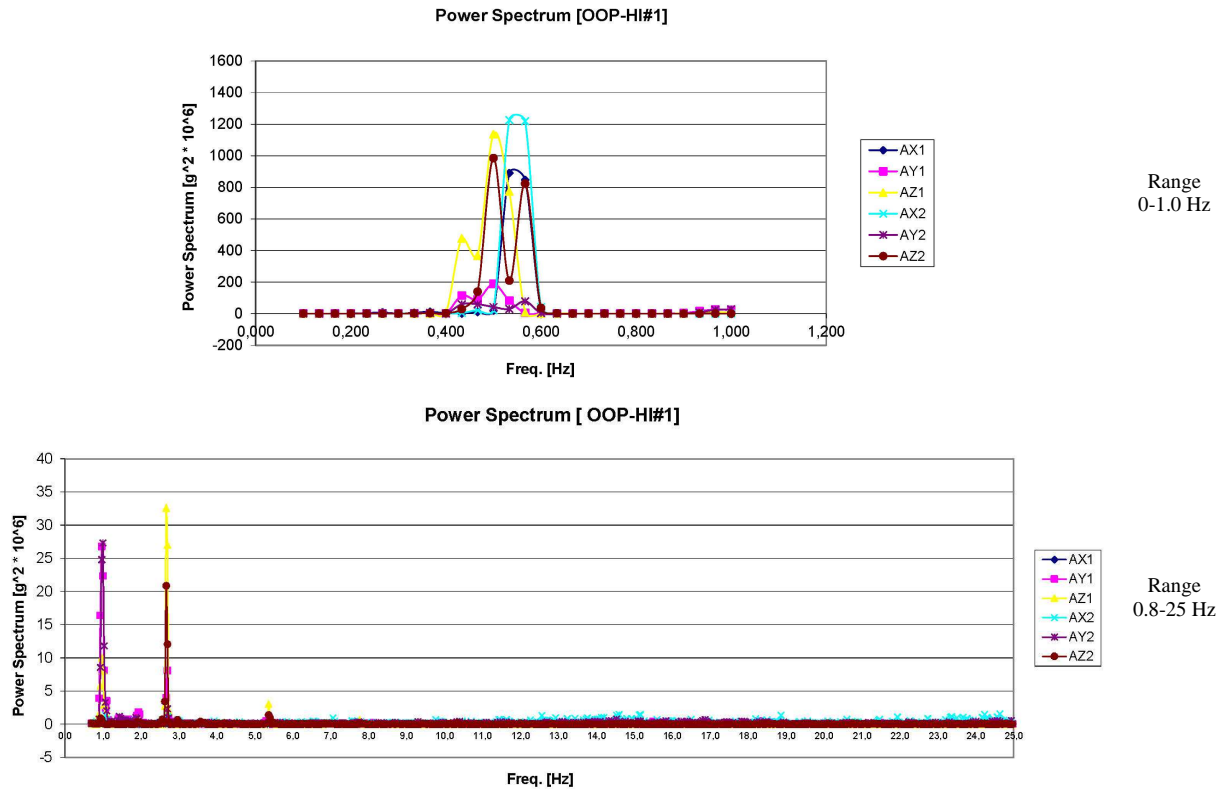


Figure 19. TSS BB - Recorded power spectrum vs. frequency. *Out-of-plane perturbation.*

The rope was the cut causing a perturbation in bending mode.

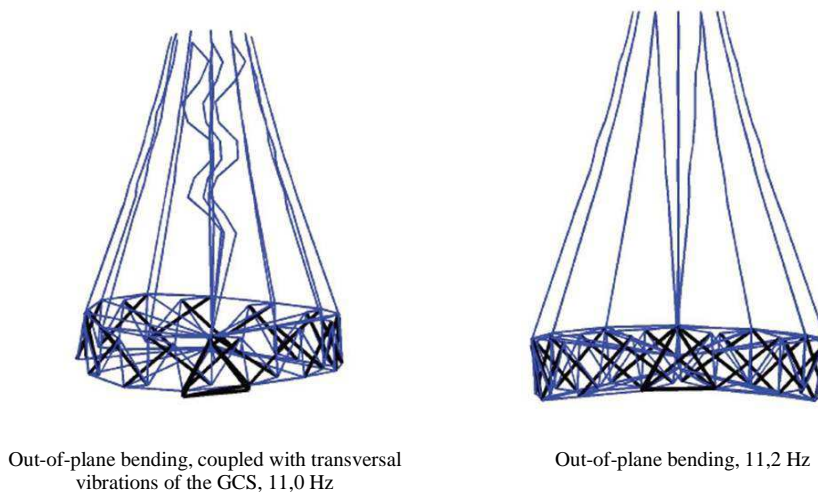


Figure 20. TSS BB - Recorded power spectrum vs. frequency. *Out-of-plane perturbation.*

In addition to the 0.5 Hz design frequency of the GCS in vertical direction, the next eight measured frequencies were at 1.2, 2.7, 5.4, 7.8, 10.3, 11.1, 13, and 13.8 Hz.

Figure 18 and Fig. 19 shows the recorded power spectrum relevant to in-plane perturbation and out-of-plane perturbation respectively.

A structural analysis was performed before and after the test campaign. Besides the frequencies relevant for the GCS, the analysis indicated that two out-of-plane natural frequencies (at, respectively, 11.0 Hz and 11.2 Hz) affected all nodes in a bending motion of the annular structure. Note that, as observed by visual inspection, the various types of modes are often coupled to each other, due to the fact that frequencies are close to each other. This can be seen for example in Fig. 20 left, where the out-of-plane bending of the TSS is coupled with the transversal vibration of the GCS supporting the IF.

The in-plane modes involve intermediate nodes only, without affecting nodes at the vertices of the base polygons. In these modes, the motion of the intermediate nodes is directed radially in the horizontal plane. The 17 calculated frequencies are in the range between 6.7 and 14.1 Hz.

The structural analysis also shows that the modes associated with the GCS correspond to the first peaks appearing in the power spectrum from the tests. The correspondence is quite clear for frequencies of about 0.5, 1.2, 2.7 Hz, and 5.4 Hz. The frequency of the first modes involving intermediate nodes (about 7, 8 and 10 Hz) are located in proximity of the peaks of the spectrum obtained from the tests. A correspondence between the frequency of the first out-of-plane bending mode at 11 Hz and relevant peak in the spectrum is also visible.

The results of the analysis are in a fairly good agreement with those of the test, even though the dynamic response of the BB appears to be coupled with that of the GCS.

A modal analysis in the absence of gravity was performed for both the BB and the FM. In both cases, the first mode is an out-of-plane cantilever-like bending mode, with frequency of 1.9 Hz for the BB and 2.1 Hz for the FM. In consideration of the fairly good agreement between tests and numerical simulations, these results show that the FM should have good dynamic performance, since its first natural frequency is not only higher than 1 Hz but indeed far away from this value.

D. Breadboard Stop-and-Go Test

This test was aimed to demonstrate the capability of the TSS BB to complete deployment even if a stop occurs during deployment. The deployment was started and stopped after 30 sec, before Phase 1 was completed (in nominal conditions, Phase 1 is completed in 2 minutes). After a 60 seconds stop, deployment was re-started until a successful completion, including Phase 2.

VI. Conclusion

The successful development of a new architectural concept of a large deployable reflector (about 12 meters in diameter) for space applications has been achieved and presented in this paper.

By exploiting “tensegrity” structural principles, a large deployable ring has been conceived, which does not include any mechanical joint or articulation between its rigid members, which are interconnected only by cables. Having no mechanical joints in the expandable ring, therefore eliminating a major potential source of single-point failures, constitutes a major advantage in terms of deployment reliability, a crucial requirement of such systems.

The new architecture has been studied in detail, and a reduced scale breadboard model (3.5 meter in diameter) has been realized and tested to validate the main design features.

Means to interface the expandable ring to the hosting spacecraft have been studied in detail, resulting in an innovative and very efficient solution.

A suitable gravity off-loading system has been designed and implemented for the test campaign of the reflector breadboard.

All major design assumptions and features have been validated during the test campaign, including notably:

- deployment functionality (including “stop-and-go” deployment verification);
- deployment accuracy / repeatability;
- stiffness in deployed configuration.

The newly conceived architecture has been protected by international patent filing, and is a potential candidate for further development studies to reach higher Technology Readiness Level (TRL) as well as, possibly, for an in-orbit deployment demonstration.

ESA has established a roadmap to increase Large Deployment Reflector TRL status⁸ and a Research and Development activity has recently started for the development of a suitable RF mesh.

References

Periodicals

- ¹Gómez Jáuregui V., “Controversial origins of tensegrity”, *Proceedings of the IASS Symposium*, 2009, Valencia, Spain, 2009, V. Domingo, A. & Lazaro, C. (ed.)
- ²Yuan, X., Peng, Z., Dong, S., Zhao, B. “A new tensegrity module - ”torus””, *Advances in Structural Engineering*, Vol. 11, 2008, pp. 243–252
- ³Tibert A. G., Pellegrino, S. “Review of form-finding methods for tensegrity structures”, *Int. J. Space Struct.*, No. 18, 2003, pp.:209–223
- ⁴Hernandez , S. J., Mirats, J. M. “Tur. Tensegrity frameworks: Static analysis review”, *Mechanism and Machine Theory*, Vol. 43, 2008, pp.859–881

Proceedings

- ⁵Oppenheim, I. J. Williams, W. O., “Tensegrity prisms as adaptive structures”, *Adaptive Structures and Material Systems*, Vol. 54, ASME, Dallas, Texas, 1997 pp. 113–120
- ⁶Peng, Z., Yuan, X., Dong, S., “Tensegrity torus”, *Proceedings of the IASS-ACPS*, Beijing, China, 2006
- ⁷Lubrano, V., Mizzoni, R., Silvestrucci, F., Raboso, D.”PIM characteristics of the large deployable reflector antenna mesh”, *4th International Workshop on Multipactor, Corona and Passive Intermodulation in Space RF Hardware*, Noordwijk, The Netherlands, 2003

Reports, Theses, and Individual Papers

- ⁸Mangenot, C., Santiago-Prowald, J., van’t Klooster, K., Fonseca, N., Scolamiero, L. et al (2010). “Large Reflector Antenna Working Group, Executive Report”, TEC-EEA/2010.636/CM, ESA, Estec, Noordwijk, The Netherlands, 2010
- ⁹Ganga, P. L., Micheletti, A., Podio-Guidugli, P., Tibert, G., ESA Study manager: Scolamiero, L., “Tensegrity Space Structures - Final Report”, KI-TSS-RP-095, ESA, Estec, Noordwijk, The Netherlands, 2011

Electronic Publications

- ¹⁰Snelson, K. D.” “Website”. URL: <http://www.kennethsnelson.net>, [cited January 2010]
- ¹¹Bob Burkhardt. “Synergetics gallery” URL.: <http://bobwb.tripod.com/synergetics/photos/index.html>, [cited January 2010].
- ¹²Harris Corporation ”Unfurlable Antenna Solutions” URL: http://download.harris.com/app/public_download.asp?fid=463 [cited March 2012]
- ¹⁵Northrop-Grumman “Astromesh©” URL: http://www.as.northropgrumman.com/products/ast_astro_mest/ [cited March 2012]

Patents

- ¹⁴Thomson, M. W., Marks, G. W., Hedgepeth, J. M., US Patent for a “Light-weight reflector for concentrating radiation”, No. 5,680,145, October 21, 1997
- ¹⁵Scolamiero, L., Zolesi, V. S., Ganga, P. L., Podio-Guidugli, P., Micheletti, A., Tibert, G., in the name of European Space Agency, International Patent for “A Deployable Tensegrity Structure, Especially For Space Applications”, Patent Application: PCT/IB2012/051309, filed March, 2012
- ¹⁶Stern, I., US Patent for a “Deployable Reflector Antenna with Tensegrity Support and Associated Method”, No. 6,542,132, April 1, 2003